CHAPTER 11

MECHANICAL PROPERTIES : HARDNESS AND COMPRESSION TESTING

CONTENTS PAGES

11.1 Introduction

Hardness is an important solid state property[1] commonly studied to determine mechanical strength and other properties of materials. It may broadly be defined as the ability of one body to resist penetration by another. All hardness tests measure some combination of various material properties, namely elastic constants[2], yield strength flow[3], plasticity[4], fracture toughness[5], state of dispersion of impurity[6], quench hardening[7], irradiation hardening[8] and grain boundary hardening[9]. Since each hardness test measures a different combination of these properties, hardness itself is not an absolute quantity and to be meaningful any statement of hardness of a body must include the method used for measurement. From time to time, attempts towards a physical definition of hardness were made[10-12]. It is now realised that hardness is not a single property but rather a whole complex of mechanical properties and at the same time, a measure of the intrinsic bonding of the material.

Point indentation techniques

(e.g. Vicker's test, Knoop test, etc.) are commonly used to study glide, defomration, anisotropy, cracks, etc. in materials. The Vicker's test is reliable for hardness measurements, since it is independent of pre-existing surface flow conditions[13], is less time consuming[14] and can yield a better statistical average with fewer indentations. Boyarskaya et al[15] reported the relation of microhar ness to load for NaCl mono-crystals. Plendl and Gielisse[16] have correlated the hardness of several crystals with their lattice energy. Julg[17] and Powarjonych[18] attempted to draw some qualitative information about the bond strength from hardness values. Katakov and Yamada[19] studied the yield strength and dislocation mobility of KCl-KBr single crystals.

Mechanical properties of stressed crystals tend to recover when they are subjected to annealing and quenching. Quenching is found to enhance hardness. The annealing, on the other hand, softens the crystal. In this chapter, investigation on the mechanical behaviour derived from the plastic deformation of RHT crystals is described and the

effect of annealing and quenching on microhardness is discussed. The results of INSTRON compression testing upto the breaking points of RHT crystals are also described.

11.2 Experimental

11.2.1 Microhardness Measurements

The grown RHT crystals with smooth surfaces and free from any microstructures were selected for their microhardness studies. Indentation studies for RHT were made on as grown (010) surfaces and on (010) freshly cleaved surfaces. The microhardness of these crystals were determined by subjecting above selected surfaces to static indentation tests in air at room temperature (300 K) using a Vicker's Microhardness Tester, Model No. 6270 (M/s. Cooke Troughton and Simms, U.K.). In this model, a Vicker's pyramidal diamond indentor is fixex to the front lens of the reproducing objective, whose optical data are those of standard 32/0.65 apochromat. The hardness tester which is provided with an optical device to indicate the testing load was attached to an incident light

microscope with the vertical illuminator replacing a standard objective.

The samples ($4 \times 3 \times 1$ mm^3) were first mounted on a flat aluminium or abonite circular disc (diameter 20 mm). The indentation marks were measured with using Filer micrometer eyepiece which resembled the standard micrometer eyepiece in design with a least count of 10 μm. Indentor load varying from 2 to 40 gms was applied for a fixed interval of time i.e. 10 sec. In another set of experiments, a constant indentor load of 15 gms was used and the period of indentation was varied from 5 to 10 sec. These experiments were repeated atleast for 10 indentation marks for each loading and each time interval on (010) as-grown and (010) cleaved surfaces. The crystals are indented at different sites such that the distance between any two indentation marks was more than five times the digonal of indentation marks to avoid surface effects due to the nearest indentation. Measurements were made on two diagonals of an indentation mark. The Vicker's Hardness Numerals (H_v) were calculated using the equation[20].

$$H_v = 1.8544 \frac{P}{d^2} \text{ kg mm}^{-2} \qquad (11.1)$$

where H_v is the Vicker's Hardness Numerals,

P is the applied indentor load in Kg, and

d is the mean diagonal length in mm.

The accuracy in the microhardness value is of the order of $\pm$ 0.2 Kg mm^{-2}. The probable error of the mean H_v was calculated based on 10 indentation mark, for a given plane and environment. But it was observed that due to slight deviation from normal incidence of the indentor on the crystal surface, two of the four vertices of the indentation marks on some of the samples were not well defined, and in such cases the measurements of lengths of diagonals were not accurate. To minimize error, half diagonals were measured. For hardness studies at different quenching temperatures, the temperature of the specimen was gradually raised and maintained at the predetermined temperature for a fixed time (more than 24 hours) and quench to room temperature. Samples were maintained at 140^{o}C for 20 hrs and cooled down to room temperature at the rate of 5^{o}C hr^{-1} in order to anneal the crystals.

11.2.2 Instron Compression Testing

For INSTRON compression testing, visible, transparent RHT crystals were selected and their dimensions were carefully determined using a travelling microscope. The crystal was placed between the two compression heads of the INSTRON machine, the upper head being slowly move downwards at an uniform speed of 0.5 cm min^{-1} and the record chart speed was 5C cm min^{-1}. The weight applied and the resulting compressions were noted on the recorded for various crystals along two directions. The compression upper head was moved until the crystal was crushed at the end of the plastic limit.

11.3 Results and Discussion

11.3.1 Microhardness Testing

Figure 11.1 shows the typical indentation mark on (010) cleaved surface with an indentor load 10 gms. The indentation mark is approximately square and have straight edges. Slip lines are observed around indentation mark. It is also

observed that the several cracks and median vents grow simultaneously from the stress concentration points, the sharp indentor edges. No preferred directions of venting were observed, as in the case of anisotropic materials, where vents tend to have a preferred orientation[21]. Even for low load, the deformation was observed to be too sever and near the indentation mark, displaced matters chipps off as observed frequently on the minerals. However, this chipping does not change the size of the indentztion mark, if diagonal ends can still be observed. The basic sequence of crack propagation events is explained as follows[22]

The sharp point of the indentor produces an inelastic deformation and at some threshold, a deformation induced flow suddenly develops into a small crack, the median vent on a plane containing the contact axis and the increase in load causes further stable growth of the median vent. On unloading, median vents begin to close but do not heal. Relaxation of deformation material within the contact zone, just before removal of the indentor superimposes intense residual tensile stresses upon the applied load, and

side wasys extending cracks, called, "laterla vents" begin to appear. The lateral vents continue to extend and cause chipping.

The plots of the square of the diagonal length of the indentation marks (d^2 in mm^2) aginst indentor load (P in gms) are illustrated in Figure 11.2. The plots are straight lines for (010) as-grown and (010) cleaved surfaces. It maybe noted that plots pass well through the origin, which indicates that the error in loading is nil in the studied range of loadings. The relation between P and d is represented by Meyer's equation :

$$P = ad^n \qquad (11.2)$$

where P is the indentor load,
d is the observed diagonal length of the indentation mark,
a is the standard hardness of the material, and
n is the Meyer index.

The value of n represents the capacity of work-hardening. Figure 11.3 shows the log log plot between $\angle_d$ and P for (010) as-grown and (010) cleaved surfaces. The slope gives the value of 'n', the Meyer index. The values of n are computed using the least square method for different loading regions and is given in Table 11.1. It is clearly seen from this table that :

(i) The work hardening exponent is greater for cleaved surfaces compared to as-grown surfaces.

(ii) The work hardening exponent is higher when the indentor load is increased.

Microhardness measurements revealed that H_v (microhardness values) is independent of loading time or dwell time, but is a function of an indentor load. The variation of H_v with indentor load for (010) as--grown and (010) cleaved surfaces is illustrated in Figure 11.4. The variation of H_v with indentor load for quenched and annealed samples is also illustrated in Figure 11.5. The following special features are noted :

Table 11.1

Meyer Index for Different Load Ranges

Load ranges p in gms.	Meyer index (work hardening exponent) n	
	(010) as grown surfaces	(010) cleaved surfaces
2-10	1.7232	1.7824
10-25	1.8317	1.8865

(i) In all cases, it is found that H_v increases with load giving a sharp maximum at 4 gms.

(ii) In all cases, consistency in H_v is revealed after 7 gms.

(iii) The absolute value of H_v in the case of quenching smaples is greater than that of the samples at room temperature and annealed crystals.

During the process of indentation the indentor penetrates to a depth comparable with, or greater than the thickness of the distored zone. Since this zone is pierced by the indentor, its effect will be marked at comparatively low loads. Consequently a noticeable increase in H_v is observed in the beginning, whence the chipping of the material from the surface is very intense. As the depth of impression of diamond pyramid increases, the effect of the distorted zone become much less prominent which explain the variation of H_v with load is almost zero beyond 8 gms load. For larger loads (beyond 16 gms) when the indentor reaches a depth at which undistorted material exists, the H_v

is independent of load.

Figure 11.5 shows that annealing decreases the hardness whereas quenching increases the hardness for all loadings of (010) cleavage surfaces. The same behaviour was also observed for (010) as-grown surfaces. They may be attributed to quenching as it introduces a large number of line and point defects and also result in creation of internal stresses. Annealing on the other hand, is a thermally activated process which leads to rearrangements of existing dislocations and other defects into low energy configurations or total or partial annhilation of these. Annealing also leads to recovery by the following mechanisms operating single or inconjuction :

(i) Vacancy migration by diffusion,

(ii) Climb of dislocation,

(iii) Polygonization,

(iv) Crystal boundary migrations and

(v) Recrystallization.

The activation energy needed for all mechanism is supplied thermally during the maintainance at elevated temperature of annealing.

Interestingly, it is observed that the RHT crystals growing at larger distance from the gel interface tend to decrease the microhardness (H_v) of the sample. This can be correlated as in the growth systems which depend on the diffusion of one reactant through a gel incorporating the other reagent, it is observed that the growth rate is greater than the gel solution interfafe, where the concentration gradients are high, away from the interface, the gradients are relatively low. Corresponding to different growth rates, the dislocation density is also different. This strongly suggests that the growth rate itself determines the number of defects grown into the crystals even in the absence of foreign impurity, this in turn affects the hardness of the crystal.

11.3.2 Instron Compression Test

The instrong compression recorder plots obtained for RHT single crystals has been

retraced and is shown in Figure 11.6. It is revealed when the crystals are pressed perpendicular to (010) and (110) as-grown faces, the Hook's law is obeyed in the complete region upto the breaking point without passing through a plastic regions before the catastrophic event. On the other hand, when crystals is pressed in a direction perpendicular to (110) cleavage plane, the crystal suffered catastrophie under a pressure by a smaller factor when compared with the dstructive forces applied to the (010) face. This difference in breaking strength (Table 11.2) observed for the cleavage plane, which has envisaged to be the hardest plane is probably to be explained by a slight deviation from the assumed perpendicular direction of the applied force causing the planes to slip. This argument can be supported by an observation made on the "crushed" crystal. After the breaking point, the crystal with its cleavage plane in contact with the compressing heads is found cleaved to thinner pieces, whereas the crystals with the other planes are just got randomly crushed into microbits.

It is attempted to compare the results

Table 11.2

Young Modulus of RHT Crystals

Plane of the crystal	Thickness (t) of the crystal in cms.	Area (A) of the crystal in cm^2	Compressibility $\Delta l \times 10^{-3}$ in cm.	Load (L) $\times 10^6$ in dynes	Strain (e) $= \frac{\Delta l}{t}$	Strain (σ) = L/A in kg cm^{-2}	Young Modulus (Y) $= \frac{\sigma \times 10^9}{e}$ dynes cm^{-2}
(010)	0.177	0.2250	6.1	10.0	0.03446	44.44	1.2894
	0.190	0.1800	3.4	4.00	0.01789	22.22	1.2417
(110)	0.131	0.1827	4.8	9.2	0.03664	51.11	1.3948
	0.151	0.1508	4.4	6.4	0.02913	42.66	1.4640

of the microhardness study with the compression testing. The inference seems to be inconcistent because of the two entirely different ways of applying pressures. These results of point indentation and compression testing differ in the damage patterns under different conditions, it is observed that : (i) (010) planes required the higher load per unit area for breaking is characterized with the smaller value of H_v and (ii) the (110) plane b having lower breaking strength exhibits the highest H_v.

11.4 Conclusions

1. RHT crystals are highly brittle, because even at low indentor loads, fracture occurs at stress concentration points.

2. Analysis of radial cracks reveal the values of fracture toughness.

3. Microhardness (H_v) values of RHT crystals is dependent on the applied indentor load but is independent of the duration of loading.

4. H_v for (010) cleaved surface is greater than that of (010) as-grown surface.

5. Quenching process increases the H_v whereas annealing decreases H_v of RHT crystals.

6. Thermal treatment influences the dislocation mobility as a result of the change in the state and distribution of point defects in the crystal lattice.

7. The work hardening exponent is higher when the indentor load is increased.

8. The work hardening exponent of (010) cleaved surface is higher than that of (010) as-grown surface.

9. Compression testing resulted in the observation of large anisotropy in breaking strength of the crystals. The cleavage plane required only a small fraction of pressure for breaking when compared with the other as-grown planes.

10. The planes with the lowest breaking

strength show the highest value of H_v and vice-versa.

11. The comparison of results of compression testing and indentation is inconclusive on account of the different mechanisms involved for the application of external forces.

12. Young modulus of RHT crystals is determined from compression testing.

REFERENCES

1. H. Buckle : Metal Rev. 4 (1959) 49.

2. J. C. Conway : J. Mater. Sci. 21 (1986) 2525.

3. E. Breval, G. C. Dodds and N. H. MacMillan : Mat. Res. Bull. 20 (1985) 731.

4. R. D. Deslattes, J. L. Targsen B. Paretzkin and A. T. Horton : J. Appl. Phys. 37 (1966) 541.

5. M. P. Horvath : J. Mater. Sci. 19 (1984) 1159.

6. G. Y. Chain : "Deformation in Ceramic Materials" (Plenum Press, N. Y., (1975).

7. J. R. Pandya and L. J. Bhagia : Ind. J. Pure & Appl. Phys. 22 (1984) 439.

8. A. R. Patel and C. C. Desai : Ind. J. Pure & Appl. Phys. 3 (1970) 1945.

9. V. K. Grigerovish : Scleromenry M Nauka, Moscow, USSR (1968) 71.

10. C. W. Stillwell : "Crystal Chemistry" (McGraw Hill Book Co. Inc., N. Y. (1938).

11. N. A. Ashby : N. Z. Engg. 6 (1951) 33.

12. A. P. Gerk : J. Mater. Sci. 12 (1977) 735.

13. T. Harnoh, H. I. Shikawa, N. Shinkari and M. Mizuhasni : J. Mater. Sci. 17 (1982) 595.

14. W. J. Weber and H. Matzke : J. Mater. Sci. 19 (1984) 2533.

15. Yu. S. Boyarskaya, Yu. P. Keldgiu, M. K. Bologa and V. V. Mendents. : Sov. Phys. Crystallogra. 14 (1969) 558.

16. J. N. Plendl and P. J. Gieliesse : Phys. Rev. 125 (1962) 828.

17. A. Julg : Phys. Chem. Miner. 3 (1978) 139.

18. A. S. Powarjonych : Z. Krist. 18 (1963) 404.

19. T. Katakov and T. Yamada : J. Appl. Phys. 16 (1977) 1119.

20. B. W. Mott : "Microindentation Hardness Testing", Butterworths, London, (1966) 9.

21. E. M. Dekker and G. D. Rieck : J. Mater. Sci. 9 (1974) 1839.

22. M. Lawn and R. Wilshaw : J. Non-Cryst. Solids 38 (1980) 391.

Captions of the figures

Figure 11.1 — Indentation marks on the (010) cleavage surface at an indentor load 10 gms.

Figure 11.2 — Variation of d^2 (square of the diagonal length of the indentation mark) with applied indentor load P.

Figure 11.3 — Meyler plot between d and P.
(⊙ -(010) as grown surface
⊡ -(010) as cleaved surface).

Figure 11.4 — Plots of Vickers Microhardness (H_v) values against applied indentor load P.
(⊙ -(010) as grown surface;
⊡ -(010) as cleaved surface)

Figure 11.5 — Graphs of Vickers microhardness (H_v) values against applied indentor load P for quenched (⊡) and annealed (●) samples.

Figure 11.6 — INSTRON - plot of applied load versus compression for (010) and (110) as-grown surfaces.

Fig. 11.1

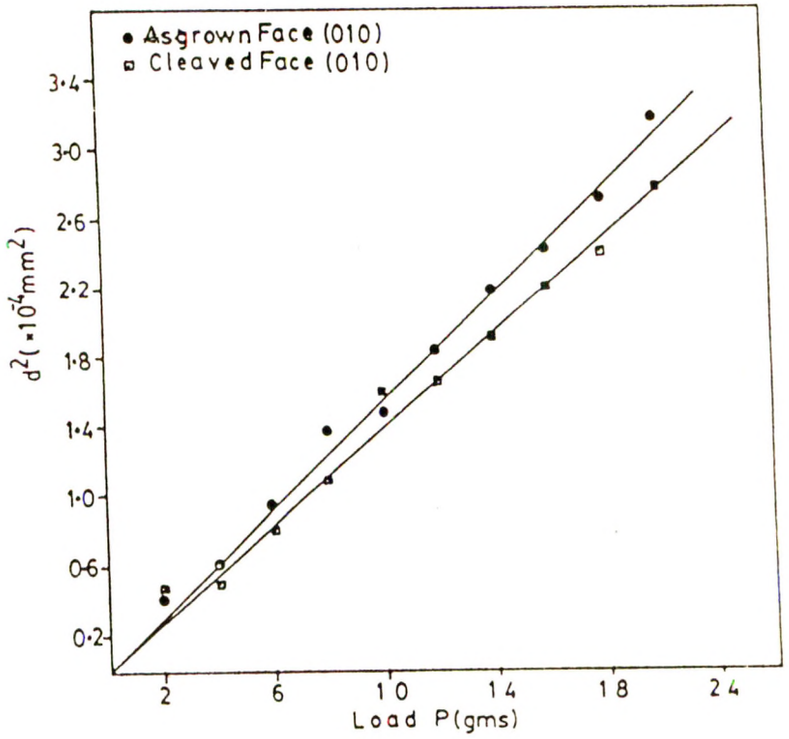

Fig. 11.2

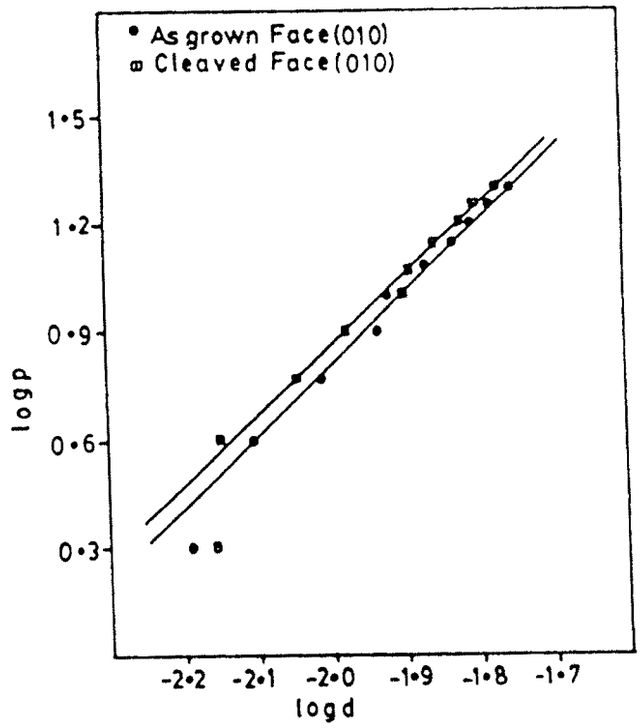

Fig. 11.3

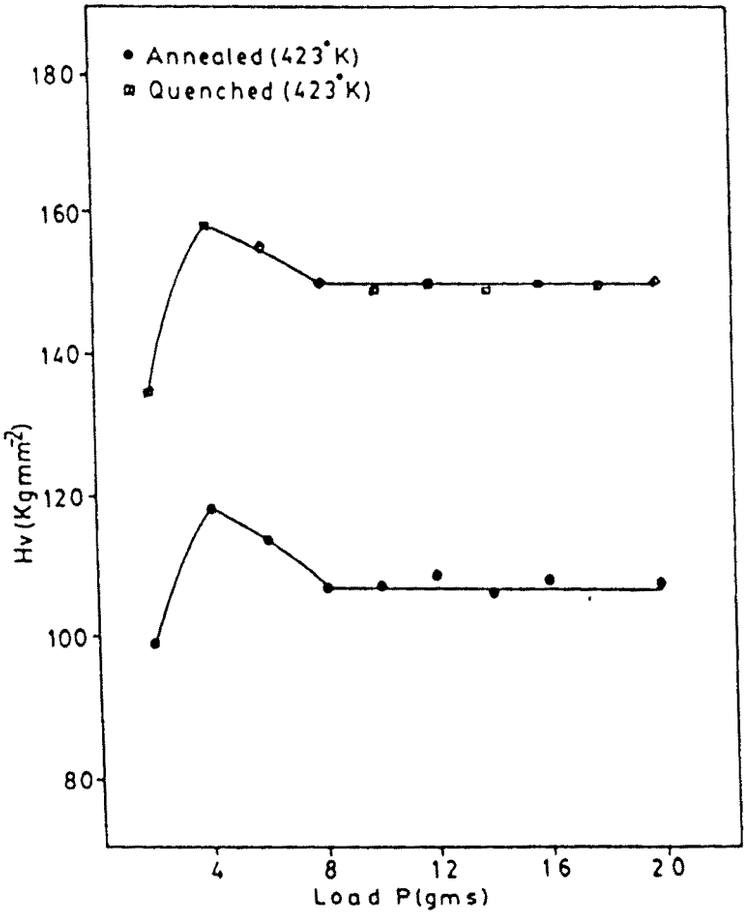

Fig. 11.4

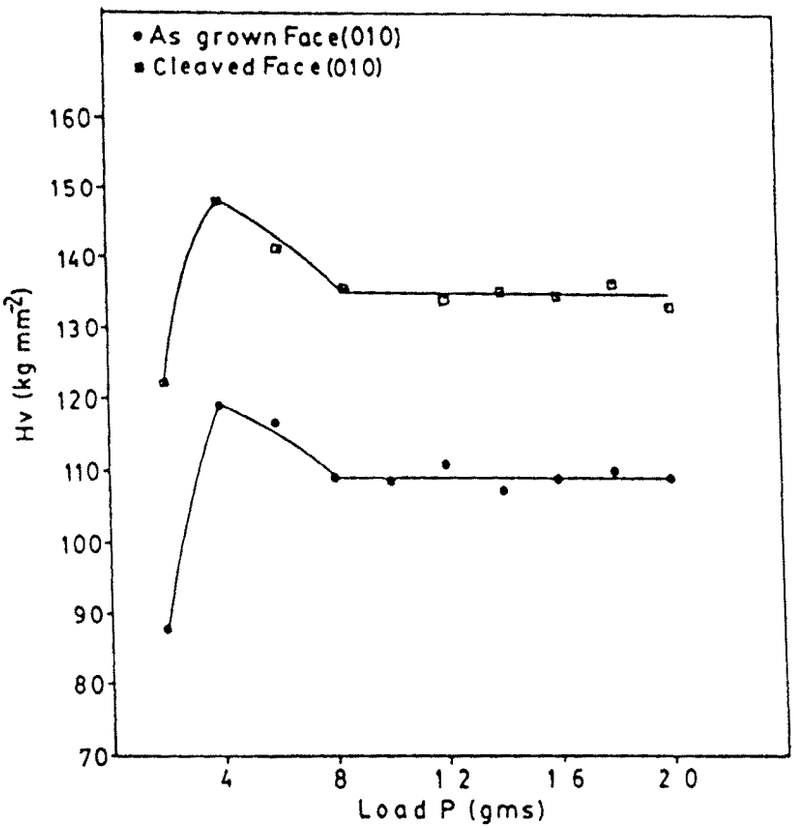

Fig. 11.5

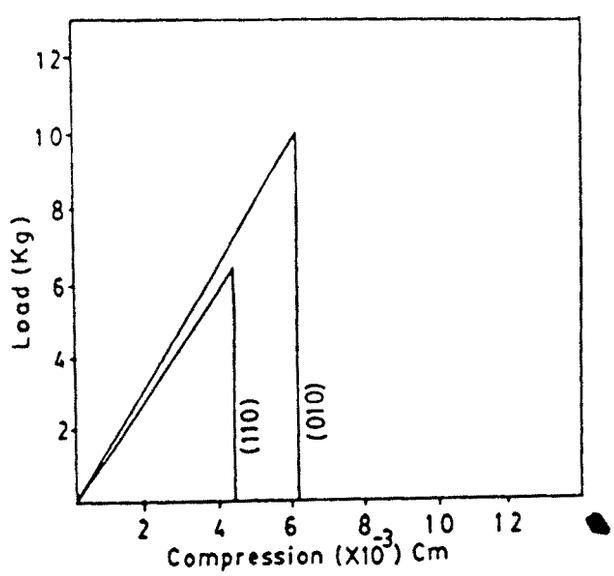

Fig. 11.6